Journal of Applied Geophysics 104 (2014) 44–57

Contents lists available at ScienceDirect

Journal of Applied Geophysics

journal homepage: www.elsevier.com/locate/jappgeo

Investigation of distribution of embedded shallow structures using the first order vertical derivative of gravity data

Tolga Gönenç

Dokuz Eylül University, Engineering Faculty, Department of Geophysical Engineering, Buca, Izmir, Turkey

ARTICLE INFO

Article history:
Received 29 June 2013
Accepted 12 February 2014
Available online 24 February 2014

Keywords:
Bouguer gravity
First order vertical derivative method
Synthetic model studies
Adala-Manisa

ABSTRACT

The utilization of the first order vertical derivative method, applied to a gravity field, in the determination of relatively low density and high density areas within the same unit can be helpful, defining such areas. In this study, the first order vertical derivative method was first applied to synthetic data and the workability of the method was investigated by creating scenarios having different densities within the same unit. Later, to compare the result of the scenarios, Adala-Manisa/Turkey and surroundings having a volcanic history were selected because of the existence of underground structures formed as a result of embedded volcanic areas. Real data set was obtained by using Scintrex CG-5 and Leica 1200 + GNSS for investigating the geological structure of the Adala-Manisa, at 400 stations. After the gravity reduction process the residual gravity anomaly values of the Adala-Manisa were obtained by removing a first order regional trend from the Bouguer gravity map. In the following process, the first order vertical derivative method was applied to the residual anomaly map. Thus, results of the synthetic anomalies and real data anomalies were compared and discussed by using the residual Bouguer gravity anomaly map. Consequently, the first order vertical derivative application in the determination of suppressed and undefinable shallow weak resources in the same media as Alluvial Fans and Alluvium units, especially on the Bouguer gravity anomaly map produces acceptable effective results.

1. Introduction

Many researchers have developed various methods based on the use of horizontal or vertical gradients of potential-field anomalies (Boschetti, 2005; Fedi and Florio, 2001; Fedi and Florio, 2013; Marcotte et al., 1992; Rao et al., 1981; Reid et al., 1990). The rationale for computing vertical gravity gradient, or a second vertical derivative, is that anomalously dense rocks occurring near the ground surface produce much stronger gradient effects than those which lie at great depths (Gupta and Grant, 1985; Gupta and Ramani, 1982; Gupta and Sutcliffe, 1990). The first derivative is a measure of slope and the second derivative is the rate of change of slope. However, it should be noted that the amplitudes of the Bouguer gravity anomalies that are caused by shallow and weak sources may be considerably smaller than those due to larger, deeply buried sources. The vertical derivative map thus enhances the weak, near-surface anomalies. Butler (1984) applied the first and second order derivative methods to gravity data. Butler indicated in his study that the first order derivatives are more sensitive and the results belonging to the second order derivative method can be used in the determination of structure place but are not suitable for any quantitative interpretation.

The first vertical derivative, a gravity field, is a transformation that is useful for the determination of shallow structures having weak density contrasts. The signatures of environments, structures, or resources having relatively lower density contrasts with the density of the general environment compared to other features having relatively high contrasts may be suppressed by signatures of features having higher density contrasts. Therefore, low density weak loose grounds or environments can be a part of this whole even if a general effect within a unit has a high density. Although materials carried by volcanic flows are the same materials in time and environmental conditions, they can create different accumulation areas with high and low densities (depending on cooling and accumulation characteristics) that have different densities but are the product of the same resource by being covered with alluvial material. Likewise, similar mechanism is dominant in places where streams, stream beds, and rivers join to the sea.

In this sense, gravity anomaly maps were prepared by creating three different synthetic model scenarios in the first phase of the study. And then, new anomaly maps were obtained by calculating the first order vertical derivative belonging to these formed anomaly maps. However, in the last phase of the model study, cross sections across different profiles were digitized in different directions by considering basic information of the scenarios (location, density, and depths of the structures) with predetermined conditions. Locations of the structures with high density contrast in these obtained cross sections, whether their geophysical indications suppress each other, and the results of the

E-mail address: tolga.gonenc@deu.edu.tr.

http://dx.doi.org/10.1016/j.jappgeo.2014.02.010
0926-9851/

first order vertical derivative method related to the difference within the frame of the scenarios formed have been discussed, and under the light of this information, assessments have been made for related area by using gravity data obtained from approximately 400 points in Adala-Manisa/Turkey.

2. Synthetic model studies

Synthetic model studies were created by using Eq. (1) (Grant and West, 1965)

$$\begin{aligned}\Delta g(x,y) = {} & \frac{B_0^0 z_0}{R^3} + 3B_2^0\Big[\left(3\cos^2\psi - 1\right)z_0^3 + \left(5\sin^2\omega\sin^2\psi - 2\cos^2\psi - 1\right)x^2 z_0 \\ & + \left(5\cos^2\omega\sin^2\psi - 2\cos^2\psi - 1\right)y^2 z_0 - 2\sin\omega\sin\psi\cos\psi\left(x^3 + xy^2 - 4xz_0^2\right) \\ & + 2\cos\omega\sin\psi\cos\psi\left(y^3 + x^2 y - 4yz_0^2\right) - 10\sin\omega\cos\psi\sin^2\psi(xyz_0)\Big]\Big/R^7 \\ & + B_2^2\Big[-3\sin^2\psi z_0^3 + \left(5\cos^2\omega - 5\sin^2\omega\cos^2\psi + 2\sin^2\psi\right)x^2 z_0 \\ & + \left(5\sin^2\omega - 5\cos^2\omega\cos^2\psi + 2\sin^2\psi\right)y^2 z_0 \\ & + 2\cos\omega\sin\psi\cos\psi\left(y^3 + x^2 y - 4yz_0^2\right) - 2\sin\omega\sin\psi\cos\psi\left(x^3 + xy^2 - 4xz_0^2\right) \\ & + 10\sin\omega\cos\omega\left(1 + \cos^2\psi\right)xyz_0\Big]\Big/R^7. \end{aligned} \quad (1)$$

If Eq. (1) is used for rectangular block with sides 2a, 2b and 2c and having a uniform density ρ;

$$B_0^0 = 8G\rho abc$$

$$B_{2=}^0 \frac{B_0^0\left(2c^2 - a^2 - b^2\right)}{6}$$

$$B_2^2 = \frac{B_0^0\left(a^2 - b^2\right)}{24}.$$

The value of ρ (the excess density or density contrast) must be assumed.

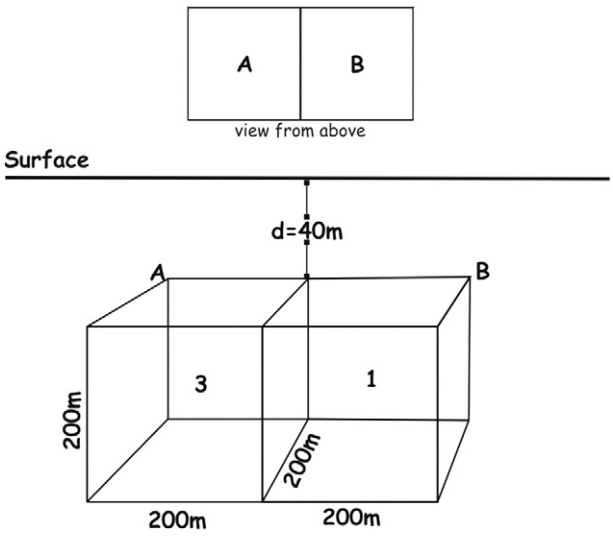

Fig. 1. General view of scenario 1.

2.1. Scenario 1

In this scenario formed by using 2 cubic (A and B) models whose density contrast is relatively higher than each other (A = 3, B = 1), locations of these cubes were designed conjointly by thinking that the same geological unit may have different density values under environmental conditions or may show lateral discontinuity. Each cube has a dimension of 200 × 200 × 200 m and a vertical discontinuity concept under the surface was formed by determining their depths from the surface as 40 m (Fig. 1).

In this sense, the effect of Cube A having higher density contrast on synthetic gravity anomaly map has highly suppressed the effect of Cube B (Fig. 2a), but the existence of the second Cube, B, is apparent in the profile P1 as a result of slight positive perturbation on the right flank of the anomaly that would be symmetrical in the absence of Cube B (Fig. 3a). However, in the first order vertical derivative map, the existence of Cube B having a lower density contrast more obvious (Fig. 2b) and also its existence is clearly reflected in a secondary positive peak superposed on the right flank of the principal derivative anomaly in the profile P1 in Fig. 3b.

2.2. Scenario 2

However, in scenario 2, 4 conjoint model cubes buried at 40 m depth below the surface and having different density contrast (A = 3, B = 1, C = 4, D = 2), but the same dimensions (200 × 200 × 200 m) are examined for their gravity effect (Fig. 4). The strong gravity signatures of Cubes A and C having relatively high densities have suppressed any indication of the presence of Cubes B and D (Fig. 5a). However, in the image of the first order vertical derivative indications related to Cubes B and D that couldn't be observed in the gravity anomaly are evident in the form of two weak, yet distinct anomalies (Fig. 5b). When profiles are taken along the lines AA^1 and BB^1, the existence of the cubes whose indications are suppressed in the gravity map becomes apparent as weak positive perturbations on the respective flanks of the prominent gravity anomalies related to the cubes having higher densities (Figs. 6a and 7a). These perturbations signaling the presence of Cubes B and D are significantly enhanced in the profiles of the first order vertical derivative (Figs. 6b and 7b).

2.3. Scenario 3

However, in the third and the last scenarios, a model including 8 cubes having different dimensions and density contrast (A = 3, B = 1, C = 4, D = 2, E = 1, F = 4, G = 2, H = 3) whose upper surfaces are all buried at a depth of 40 m was designed (Fig. 8). The dominant effects of this last model were reflected on gravity anomaly results (Fig. 9a) which is suppressed by Cubes A, F and C in total on the result. However, signatures related to cubes A, B, C, D, F, G, and H have become apparent in the image of the first order vertical derivative anomaly (Fig. 9b), once again any indication of Cube E cannot be observed. Although gravity signatures related to individual cubes, with the exception of that related to Cube H, are not discernible in the profile P1 along the line AA^1 (Fig. 10a), they are observed in a relatively definable manner in the profile P1 derived from the first order vertical derivative anomaly map (Fig. 10b). However, the existence of Cube E having a low density value is expressed only by a very slight difference in the steepness of the left flank of the principal peak anomaly, highlighted by a red circle. In effect, without knowledge of the existence of Cube E, this slight difference would go unnoticed. Cubes that have limited or indiscernible expression in gravity profiles extracted from the cubes that have limited or indiscernible expression in gravity profiles extracted from the synthetic gravity anomaly image along the lines BB^1 and CC^1 (Figs. 11a and 12a) yield stronger signatures in the profiles of the first order vertical derivative but nevertheless expressions of cubes having very low densities couldn't be observed (Figs. 11b and 12b).